Nonequilibrium Cell Model for Multicomponent (Reactive) Separation Processes

Arnoud Higler
Dept. of Chemical Engineering, Clarkson University, Potsdam, NY 13699

R. Krishna
Dept. of Chemical Engineering, University of Amsterdam, 1018 WV, Amsterdam, The Netherlands

Ross Taylor
Dept. of Chemical Engineering, Clarkson University, Potsdam, NY 13699 and
Dept. of Chemical Engineering, University of Twente, 7500 AE, Enschede, The Netherlands

A generic nonequilibrium cell model for multicomponent separation processes, including liquid-phase chemical reactions, was developed. Its important features include the use of Maxwell-Stefan equations to describe interphase mass transfer and the use of a multiple cell per stage approach to consider various mixing characteristics of vapor and liquid phases. A finite difference approach was used for solving the diffusion-reaction equations in each fluid phase to properly account for effects of reactions on mass transfer. The multiple cells per stage approach was adopted to take into account the effect of concentration and temperature profiles on a tray on the local reaction rates. The model was compared to several case studies by Kooijman (1995). Comparison of various flow models showed only minor differences between Kooijman's model and the nonequilibrium cell model. The differences were found only for cases in which the phases are assumed to be imperfectly mixed and to be caused by different ways of modeling the interface concentration profiles in various flow models. In addition, some calculations are described for reactive distillation operations described by Okasinski and Doherty (1998) and Marek (1956). These examples show that staging in both flow directions influences overall column performance considerably.

Introduction

For over a hundred years, methods and models for calculation of steady-state stagewise equation processes have been proposed and used by several generations of engineers. Sorel (1899) describes a simple steady-state distillation column based on the assumption that every stage operates at equilibrium. The early 1920s saw the development of two graphical methods: the Ponchon-Savarit (1921) method and the (McCabe-Thiele (1925) method. Ponchon-Savarit methods have now largely been replaced by computer methods, but the McCabe-Thiele method is still used in many chemical engineering curricula, because it is so illustrative of the concepts of stagewise separation processes.

With the advent of computers, a large number of methods was developed for solving Sorel's equations numerically. An excellent review of the field is by Seader (1985). More powerful computers have allowed the development of models of increasing complexity and accuracy. Sorel's equations are based on the assumption that the vapor and liquid flows that leave a stage are in thermodynamic equilibrium. In actual columns, however, stages rarely operate at equilibrium. Often these deviations from equilibrium are accounted for by the incorporation into the model of efficiency factors. Extensive discussions of the drawbacks encountered when using ef-

ficiencies are given by Krishnamurthy and Taylor (1985) and by Seader (1989).

Nonequilibrium modeling

To circumvent many of the problems related to the use of efficiencies, a nonequilibrium stage model was developed by Krishnamurthy and Taylor (1985). Nonequilibrium models do not use efficiencies, since mass-transfer rates are calculated directly from fundamental mass-transfer models. The model that was presented by Krishnamurthy and Taylor (1985) consists of a set of mass and energy balances for the vapor and liquid phases, along with rate equations for the evaluation of mass- and heat-transfer rates. The assumption of phase equilibrium is made only at the vapor-liquid interface. The method proposed by Krishnamurthy and Taylor requires the evaluation of the mass-transfer processes for both phases separately. These mass-transfer processes are linked together by the fact that the mass-transfer rates at the vapor liquid interface should be the same for both phases. This suggests that one could also write one mass-transfer relation, using an overall mass-transfer coefficient and the average concentration gradient between bulk liquid and bulk vapor phase. This approach is not recommended by Kooijman and Taylor (1995), who found cases in which the use of overall mass-transfer coefficients will result in components moving in the wrong direction. This is because the use of overall mass-transfer coefficients is only justified if the partial molar enthalpies are all equal (equimolar overflow) *and* if there is no sensible heat transfer between the two phases.

An attempt was made by Krishnamurthy and Taylor (1985) to take into account flow patterns on distillation trays by imposing particular concentration profiles over the flow path lengths in both phases. Based on the particular assumed concentration profile, an average concentration for both phases can be calculated. The average mass-transfer rate can then be evaluated using the binary mass-transfer coefficients and the average (arithmetic or logarithmic) composition difference. The overall mass-transfer rate is calculated by multiplying the average mass-transfer flux by the interfacial area on the stage. Kooijman and Taylor (1995) point out that although the assumption of concentration profiles along the flow paths might lead to seemingly good results, the method itself is fundamentally wrong. They went on to develop a method in which the mass-transfer calculations for both phases are done independently. Assuming various flow models for vapor and liquid flow (plug flow, ideally mixed flow, and axially dispersed flow), they derive expressions for the mass-transfer rates in the various flow types. This method is more sound than the approach taken by Krishnamurthy and Taylor, but it still requires one to make some assumptions that limit the flexibility of the model and, for the liquid plug-flow model, one is required to specify a correction factor for the vapor interface concentration.

In recent years, various nonequilibrium models for reactive distillation have been presented (Sundmacher and Hoffmann, 1994; Sundmacher, 1995; Kreul et al., 1999, Higler et al., 1998, 1999a). All these models use the Maxwell-Stefan theory for mass transfer, and mainly differ in the way that the reaction is implemented. Sundmacher (1995) and Sundmacher and Hoffmann (1994) present an extensive study on the production of MTBE by means of reactive distillation. The model is used for description of a laboratory-scale column, and assumes pseudo-homogeneous kinetics. Kreul et al. (1999) present a model for homogeneous reactive distillation in a packed column. All of these models are developed for packed columns, and, therefore, do not consider liquid backmixing on distillation trays.

A drawback of nonequilibrium models is that they require information about the column configuration. This is needed to calculate model parameters such as the mass- and heat-transfer coefficients. The latter ones usually are obtained from semi-empirical correlations. The computed solution of the model equations, therefore, depends to a certain extent on the quality of the correlations. Much of the opposition to nonequilibrium models was, and still is, based on this issue. Nevertheless, nonequilibrium models are gaining more and more ground at the expense of the conventional equilibrium stage models (see, for example, Kreul et al., 1999; Higler et al., 1998, 1999a,b; Lee and Dudukovic, 1999). Taylor et al. (1992) state that nonequilibrium models are particularly useful for modeling operations (1) in packed columns; (2) involving strongly nonideal systems, (3) involving systems with trace components (4) in columns with profiles that exhibit maxima or minima, and (5) where efficiencies are unknown.

For systems with chemical reactions, residence time distribution will be important, as well as a proper description of mass transfer. The reaction rates and chemical equilibrium constants are dependent on the local concentrations and temperature and may, therefore, vary along the flow path of liquid on a tray. In addition, if the reaction is fast enough, there will be an interaction between mass transfer and reaction. This cannot be described correctly when using the method proposed by Kooijman and Taylor (1995).

Flow on distillation trays

It has long been recognized that liquid staging results in improved performance of a distillation tray. Because a liquid is never perfectly mixed on a distillation tray, concentration profiles along the liquid flow path will arise in the liquid phase under the influence of mass transfer. If there is no horizontal vapor mixing, this will cause concentration profiles in the vapor flow leaving the stage. Consequently, the overall tray efficiency will be higher than the Murphree Point efficiency (see Lockett, 1986). Lewis (1936) derived an expression for the maximum achievable tray efficiency as a function of the point efficiency, assuming there is no liquid backmixing. In reality, the tray efficiency will fall short of the maximum achievable efficiency due to various nonidealities in the flow pattern. These may be caused by liquid backmixing, horizontal vapor mixing, nonuniform liquid flow across the tray, nonuniform vapor flow through the tray, and entrainment and weeping. This article is focused on the first point, although the outlined methodology allows for studying of all of these issues.

Liquid backmixing occurs mainly due to two mechanisms: Turbulence in the liquid continuous region, and motion of liquid droplets in the vapor continuous region (Bennett and Grimm, 1991). A first study on liquid backmixing on distillation trays was presented by Kirschbaum (1948), who compares flow on a distillation tray to flow through a cascade of perfectly mixed pools of liquid. Gautreaux and O'Connell

(1955) used the liquid mixing pool concept to derive an expression relating the point efficiency to the plate efficiency. Wijn (1996) used a cell model to study the influence of downcomer layout patterns on the tray efficiency. Alejski (1991) presented an equilibrium stage model, in which the liquid phase is split up in a number of equilibrium cells along the liquid flow path to account for backmixing in a reactive distillation column. Point efficiencies were used to take into account mass transfer in the equilibrium cells.

In all of the above studies a liquid mixing pool concept is used to determine the effect of staging in the liquid flow direction. Quantification of backmixing usually is done by means of eddy diffusion models (such as Bennett and Grimm, 1991; Raper et al., 1984; Barker and Self, 1962; Sohlo and Kinnunen, 1977). These models assume that the axial spreading of a tracer in the liquid flow (z) direction on a distillation tray can be described by

$$\frac{1}{Pe}\frac{\partial^2 x}{\partial z^2} - \frac{\partial x}{\partial z} = 0 \tag{1}$$

in which x is the mole fraction of the tracer and z is the axial coordinate. The Peclet number Pe is given by

$$Pe = \frac{u^L \cdot l}{D_e} \tag{2}$$

D_e is the eddy diffusion coefficient, l is the flow path length (m), and u^L is the superficial liquid velocity (m·s^{-1}) on a stage. Important limitations of the eddy diffusivity model are that it only applies to isotropic liquid flow, and, therefore, that it cannot be used for description of circulation patterns at, for instance, the column wall or the outlet weir. A summary of estimation methods for the axial dispersion coefficient is given by Lockett (1986) and Bennett and Grimm (1991). Most of these methods are curve fits to experimental data in which a functional dependence is assumed with respect to parameters such as the vapor and liquid flows and the liquid holdup. The method of Bennett and Grimm (1991) is based on a drop trajectory model.

The Peclet number for the axially dispersed flow model can be related to a number of well-mixed liquid pools in the liquid flow direction N by the following equation

$$\frac{1}{N} = \frac{2}{Pe} - \frac{2}{Pe^2}\left[1 - \exp\left(-Pe\right)\right] \tag{3}$$

Model Formulation

In this article a nonequilibrium mixing pool concept will be used to describe the mass transfer/reaction/flow problem. The two-phase mixture on a tray is split up in a number of contacting cells, for each of which mass and energy balances can be written, along with mass-transfer rate equations. A representation (side view) of a general stage j is given in Figure 1. Stage numbering in a column is from top to bottom. (Figure 1 also serves as an introduction to the notation used in this article.) L_j^S and V_j^S (mol·s^{-1}) represent the liquid and
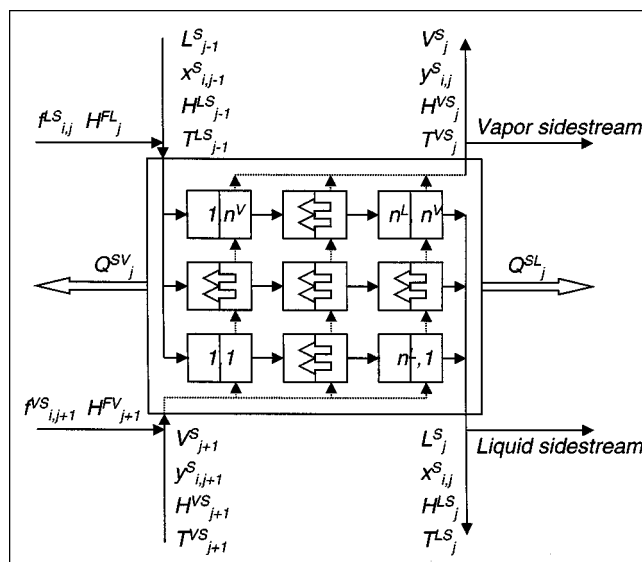
Figure 1. Model stage.

vapor molar flow rates from stage j, respectively. The mole fractions of component i in the liquid and vapor streams are denoted by $x_{i,j}$ and $y_{i,j}$, and H_j^{LS} and H_j^{VS} (J·mol^{-1}) represent the enthalpies of the liquid and vapor streams leaving stage j. T_j^{LS} and T_j^{VS} are the temperatures of the streams leaving stage j. $f_{i,j+1}^{VS}$ is the vapor feed rate of component i to stage $j+1$, and $f_{i,j}^{LS}$ is the liquid feed rate of component i to stage j. Q_j^{VS} and Q_j^{LS} are external heat duties that may be specified to either phase of stage j. The cell numbering is also illustrated in Figure 1. n^V is the number of cells in a vapor flow path, and n^L is the number of cells in a liquid flow path. Cell numbering is from left to right and from bottom to top. The stage equations will be treated first and, subsequently, the equations for each cell.

Stage equations

The overall mass balances for each stage, for the liquid and vapor phase, are given by

$$\left(1 + r_j^L\right) \cdot L_j^S - \sum_{k=1}^{n^V} L_{(n^L,k)}^C - F_j^{LS} = 0 \tag{4}$$

$$\left(1 + r_j^V\right) \cdot V_j^S - \sum_{k=1}^{n^L} V_{(k,n^V)}^C - F_{j+1}^{VS} = 0 \tag{5}$$

Here r_j^V and r_j^L are the vapor and liquid sidestream ratios. These are nonzero only if a sidestream is specified to stage j. $V_{(k,n^V)}^C$ is the vapor flow (mol·s^{-1}) coming from the kth cell in the top row of cells in the nonequilibrium stage, and $L_{(n^L,k)}^C$ is the liquid flow rate (mol·s^{-1}) from the kth cell in the last column of cells in the nonequilibrium stage (see Figure 1). F_j^L and F_{j+1}^V are the overall liquid and vapor feed rates (mol·s^{-1}) to stage j and $j+1$, respectively. The vapor feed to stage $j+1$ is added to stage j, as it is assumed that the vapor fraction of a feed goes up instantly and does not interfere with the tray below.

The stage component balance equations for the liquid and vapor phase are given by

$$\left(1 + r_j^L\right) \cdot x_{i,j}^S \cdot L_j^S - \sum_{k=1}^{n^V} x_{i,(n^L,k)}^C \cdot L_{(n^L,k)}^C - f_{i,j}^{LS} = 0 \quad (6)$$

$$\left(1 + r_j^V\right) \cdot y_{i,j}^S \cdot V_j^S - \sum_{k=1}^{n^L} y_{i,(k,n^V)}^C \cdot V_{(k,n^V)}^C - f_{i,j+1}^{VS} = 0 \quad (7)$$

$x_{i,(n^L,k)}^C$ and $y_{i,(k,n^V)}^C$ are the liquid- and vapor-phase mole fractions leaving cell k. $f_{i,j+1}^{VS}$ is the vapor feed rate $(\text{mol} \cdot \text{s}^{-1})$ of component i to stage $j+1$ and $f_{i,j}^{LS}$ is the liquid feed rate $(\text{mol} \cdot \text{s}^{-1})$ of component i to stage j. The stage energy balances are given by

$$\left(1 - r_j^L\right) \cdot H_j^{LS} \cdot L_j^S - \sum_{k=1}^{n^V} H_{(n^L,k)}^{LC} \cdot L_{(n^L,k)}^C - F_j^{LS} H_j^{FL} + Q_j^{LS} = 0$$

$$(8)$$

$$\left(1 + r_j^V\right) \cdot H_j^{VS} \cdot V_j^S - \sum_{k=1}^{n^L} H_{(k,n^V)}^{VC} \cdot V_{(k,n^V)}^C - H_{j+1}^{FV} F_{j+1}^V$$

$$+ Q_j^{VS} = 0 \quad (9)$$

$H_{(n^L,k)}^{LC}$ and $H_{(k,n^V)}^{VC}$ are the enthalpies $(\text{J} \cdot \text{mol}^{-1})$ of the streams leaving the appropriate cells on the stage. H_{j+1}^{FV} is the vapor-phase enthalpy $(\text{J} \cdot \text{mol}^{-1})$ of the feed to stage $j+1$, and H_j^{FL} is the enthalpy $(\text{J} \cdot \text{mol}^{-1})$ of the liquid feed to stage j. The stage equations are completed by the stage hydraulic equation

$$p_j - p_{j-1} - \left(\Delta p_{j-1}\right) = 0 \quad (10)$$

where p_j and p_{j-1} are the stage pressures (Pa) on stages j and $j-1$, respectively. Δp_{j-1} is the pressure drop per tray from stage $j-1$ to stage j. The pressures in all cells on a stage are assumed to be equal to the stage pressure. The pressure drop over the stage is considered to be a function of the stage flows, the fluid properties, and the equipment layout parameters.

Cell equations

A representation of a contacting cell is given in Figure 2. It is assumed that the bulk of both vapor and liquid are perfectly mixed and that the resistances to mass transfer are located in two films at the vapor/liquid interface. Figure 2 also serves to introduce the notation used for the cell equations. $L_{(k,m)}^C$ and $V_{(k,m)}^C$ are the liquid and vapor flow rates from cell (k,m). $x_{i,(k,m)}^C$ and $y_{i,(k,m)}^C$ are the compositions of the liquid and vapor streams leaving the cell, and $T_{(k,m)}^{LC}$ and $T_{(k,m)}^{VC}$ are the vapor and liquid temperatures (K). The enthalpies of the vapor and liquid streams leaving the cell are denoted by $H_{(k,m)}^{VC}$ and $H_{(k,m)}^{LC}$. $\mathfrak{N}$ represents the mass-transfer rate $(\text{mol} \cdot \text{s}^{-1})$, and $\mathcal{E}$ the energy transfer rate $(\text{J} \cdot \text{s}^{-1})$.

$f_{i,(k,m)}^{LC}$ and $f_{i,(k,m)}^{VC}$ are the liquid and vapor feed rates of component i to cell (k,m). $H_{(k,m)}^{FL}$ and $H_{(k,m)}^{FV}$ are the feed
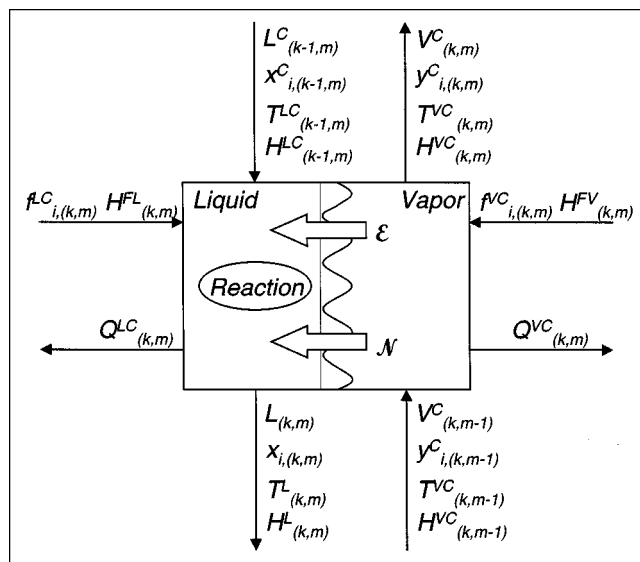

Figure 2. Nonequilibrium cell.

enthalpies for the liquid and vapor phases, respectively. $Q_{(k,m)}^{LC}$ and $Q_{(k,m)}^{VC}$ are external heat duties $(\text{J} \cdot \text{s}^{-1})$ that may be specified to the cell.

A few remarks need to be made here with respect to the feed streams and heat duties. In the presented model, one has the option to specify the feeds to either the cells or the stage under consideration. In a real column, feeds are supplied to a column between two stages, in such a way, that the liquid part of the feed is preferably equally distributed over the tray. The vapor fraction of the feed goes up instantly and does not normally interfere with the tray below. Thus, in most cases, the vapor feed stream should be added to the stage flow leaving the feed stage. This means the the vapor feeds will normally be treated in Eqs. 5, 7 and 9, rather than in cell Eqs. 12, 16 and 18. Since the liquid is normally distributed over the stage, the liquid will enter the cells directly, and the feed flows should be added to the cell Eqs. 11, 15, and 17, rather than Eqs. 4, 6 and 8. However, all this depends on the configuration used.

Similar considerations apply to the heat duties. Depending on the configuration used, they may be specified for individual cells or to the streams leaving the stages.

The total mole (mass) balances for the liquid phase and vapor phase in the contracting cell are given by

$$L_{(k,m)}^C - L_{(k-1,m)}^C - F_{(k,m)}^{LC} - \mathfrak{N}_{t,(k,m)}^L$$

$$+ \sum_{l=1}^{r} \left(\sum_{i=1}^{c} \nu_{i,l} \right) R_{l,(k,m)} \epsilon_{(k,m)} = 0 \quad (11)$$

$$V_{(k,m)}^C - V_{(k,m-1)}^C - F_{(k,m)}^{VC} + \mathfrak{N}_{t,(k,m)}^V = 0 \quad (12)$$

$F_{(k,m)}^{LC}$ and $F_{(k,m)}^{VC}$ represent the total liquid and vapor feed stream to cell (k,m). $\mathfrak{N}_{t,(k,m)}^L$ and $\mathfrak{N}_{t,(k,m)}^V$ are the total mass-transfer rates in vapor and liquid phase. The total mass-transfer rates are obtained by summing up over the in-

dividual component mass-transfer rates

$$\mathfrak{N}_{t,(k,m)}^{L} = \sum_{i=1}^{c} \mathfrak{N}_{i(k,m)}^{L} \qquad (13)$$

$$\mathfrak{N}_{t,(k,m)}^{V} = \sum_{i=1}^{c} \mathfrak{N}_{i,(k,m)}^{V} \qquad (14)$$

$R_{l,(k,m)}$ represents the reaction rate (mol·m^{-3}·s^{-1}) of reaction l in cell (k,m). $\nu_{i,1}$ is the stoichiometric coefficient of component i in reaction l. $\epsilon_{(k,m)}$ is a specific reaction volume (m^{3}). For homogeneous reactions, this is the total liquid inventory in the cell. For heterogeneous reactions, it is the total catalyst volume present in the cell. Stage number indices have been dropped here for clarity.

The conservation equations for each component in both phases are given by

$$L_{(k,m)}^{C} \cdot x_{i(k,m)}^{C} - L_{(k-1,m)}^{C} \cdot x_{i,(k-1,m)}^{C} - f_{i,(k,m)}^{LC} - \mathfrak{N}_{i,(k,m)}^{L}$$

$$+ \sum_{l=1}^{r} \nu_{i,l} R_{l,(k,m)} \epsilon_{(k,m)} = 0 \quad (15)$$

$$V_{(k,m)}^{C} \cdot y_{i,(k,m)}^{C} - V_{(k,m-1)}^{C} \cdot y_{i,(k,m-1)}^{C} - f_{i,(k,m)}^{VC} + \mathfrak{N}_{i,(k,m)}^{V} = 0$$

$$(16)$$

Indexing is for a general cell. However, not all cells receive a flow from a previous cell: The cells in the column on the lefthand side of Figure 1 receive their liquid feed from the stage above. The liquid flow to these cells is therefore the stage flow from the stage above multiplied by a splitting factor. For simplicity, we choose this splitting factor to be the $1/n^{V}$. Similar considerations apply to the bottom row of cells with respect to the vapor flow rate. Here the splitting factor is taken to be $1/n^{L}$.

The energy conservation equations for both phases in cell (k,m) are given by

$$L_{(k,m)}^{C} \cdot H_{(k,m)}^{LC} - L_{(k-1,m)}^{C} \cdot H_{(k-1,m)}^{LC} - F_{(k,m)}^{LC} H_{(k,m)}^{FL} + Q_{(m,k)}^{LC}$$

$$- \mathcal{E}_{(k,m)}^{L} = 0 \quad (17)$$

$$V_{(k,m)}^{C} \cdot H_{(k,m)}^{VC} - V_{(k,m-1)}^{C} \cdot H_{(k,m-1)}^{VC} - F_{(k,m)}^{VC} H_{(k,m)}^{FV} + Q_{(m,k)}^{VC}$$

$$+ \mathcal{E}_{(k,m)}^{V} = 0 \quad (18)$$

$\mathcal{E}_{(k,m)}^{L}$ and $\mathcal{E}_{(k,m)}^{V}$ are the liquid and vapor phase energy transfer rates, respectively. These should be the same for both phases. An extra reaction term is not required in the energy balances, because this is directly accounted for by the individual component enthalpies.

Transport relations

The mass-transfer rates in the above conservation equations are calculated by means of the Maxwell-Stefan theory (see Krishna and Wesselingh, 1997; Taylor and Krishna, 1993). The Maxwell-Stefan equations for the liquid and vapor phase, respectively, are given by Eqs. 19 and 20. Cell and stage indices have been dropped for clarity

$$\frac{x_i}{\mathfrak{R} T} \frac{\partial \mu_i^{L}}{\partial \eta} = \sum_{j=1}^{c} \frac{x_i \mathfrak{N}_j^{L} - x_j \mathfrak{N}_i^{L}}{c_t^{L} \kappa_{i,j}^{L} a} \qquad (19)$$

$$\frac{y_i}{\mathfrak{R} T} \frac{\partial \mu_i^{V}}{\partial \eta} = \sum_{j=1}^{c} \frac{y_i \mathfrak{N}_j^{V} - y_j \mathfrak{N}_i^{V}}{c_t^{V} \kappa_{i,j}^{V} a} \qquad (20)$$

where $\mathfrak{R}$ is the gas constant (J·mol^{-1}·K^{-1}) μ_i is the chemical potential (J·mol^{-1}) of species i, η is a dimensionless film coordinate, c_t^{L} is the total liquid phase concentration (mol·m^{-3}) and c_t^{V} is the total vapor-phase concentration (mol·m^{-3}). $\kappa_{i,k}^{L} a$ and $\kappa_{i,j}^{V} a$ are the liquid- and vapor-phase volumetric mass-transfer coefficients, respectively. Only $c-1$ of these equations are independent. The mole fraction of the cth component is obtained by the summation equations for both phases

$$\sum_{i=1}^{c} x_i - 1 = 0 \qquad (21)$$

$$\sum_{i=1}^{c} y_i - 1 = 0 \qquad (22)$$

In addition, for a homogeneous system, the mass-transfer rates in the liquid mass-transfer film may change due to the chemical reaction

$$\frac{\partial \mathfrak{N}_i^{L}}{\partial \eta} = a \cdot \delta^{L} \sum_{l=1}^{r} \nu_{i,l} R_l \qquad (23)$$

For most systems in reactive distillation, this term is fairly small. For systems with low Hatta numbers, this term will not be very important. However, it will not always be clear in advance in which regime a stage will be operating, and this may even vary from stage to stage.

In their article Krishnamurthy and Taylor (1985), and later Kooijman (1995), rewrite the generalized Maxwell-Stefan (GMS) equations into an expression for a mass-transfer coefficient multiplied by a driving force to obtain an expression for the mass-transfer rate directly. However, this is not usually possible in systems with liquid film reactions. Equations 19 and 23 form a system of highly nonlinear coupled differential equations that cannot be solved analytically in general, and we will have to rely on numerical techniques. Since concentration gradients within the diffusion layers on either side of the vapor-liquid interface in distillation operations are not usually steep, a finite difference approximation can be used with a reasonably small number of grid points, so that calculation cost should not become too much of a problem. For fast reactions, the use of more grid points is advisable.

Finite differencing the Maxwell-Stefan equations is done by dividing the mass-transfer film in discrete steps by means of a number of grid points. The differential terms from Eq. 19 and Eq. 20 are approximated by

$$\left(\frac{x_i}{\mathfrak{R} T} \frac{\partial \mu_i}{\partial \eta} \right)_n = \sum_{j=1}^{c-1} (\Gamma_{i,j})_n \frac{(x_j)_n - (x_j)_{n-1}}{\Delta \eta} \qquad (24)$$

in which

$$\Gamma_{i,j} = \delta_{i,j} + x_i \cdot \left(\frac{\partial \ln(\gamma_i)}{\partial x_j} \right)_{T,P,x_k,k \neq j = 1 \dots n-1} \quad (25)$$

Central difference approximations should not be used here, since they have a tendency to generate zigzag-profiles. Using the above discretization scheme does not generate these problems, but results in the introduction of a numerical diffusion term. However, since in all but some very rare cases the concentration profiles will be nearly linear, this term is not expected to have that much of an impact.

The energy transfer rates consist of convective and conductive contributions. For the liquid and vapor phases

$$\mathcal{E}_k^L = -h^L \cdot a \cdot \frac{\partial T^L}{\partial \eta} + \sum_{i=1}^{c} \mathfrak{N}_i^L \mathfrak{K}_i^L \quad (26)$$

$$\mathcal{E}^V = -h^V \cdot a \cdot \frac{\partial T^V}{\partial \eta} + \sum_{i=1}^{c} \mathfrak{N}_i^V H_i^V \quad (27)$$

Here h^L and h^V are the heat-transfer coefficients ($J \cdot K^{-1} \cdot m^{-2} \cdot s^{-1}$) for liquid and vapor phase. Derivatives in the energy transfer equations are in the calculation replaced by central difference approximations.

Interface equations

We assume physical equilibrium at the vapor liquid interface. For each component, we have

$$y_i^I - K_i x_i^I = 0 \quad (28)$$

Here y_i^I is the vapor-phase composition at the interface and x_i^I is the liquid-phase composition at the interface. K_i is the vapor-liquid equilibrium ratio for component i and is a function of interface temperature (T^I) and concentrations and the stage pressure (p_j)

$$K_i = K_i\left(x_i^I, y_i^I, T^I, p_j \right) \quad (29)$$

In addition, it is necessary that all the mole fractions should sum up to one for both phases

$$\sum_{i=1}^{c} x_i^I - 1 = 0 \quad (30)$$

$$\sum_{i=1}^{c} y_i^I - 1 = 0 \quad (31)$$

From a mass and energy balance over the interface, it follows that the mass and energy transfer rates through the interface should be continuous, which leads to the following equations

$$\mathfrak{N}_i^L |_I = \mathfrak{N}_i^V |_I \quad (32)$$

For the energy transfer rate

$$\mathcal{E}^L |_I = \mathcal{E}^V |_I \quad (33)$$

This equation plays a very important role in determining the mass-transfer rates. The Maxwell-Stefan equations by themselves are floating equations. They relate the driving force for mass transfer of a component to the frictional drag between different species. Equation 33 is, therefore, required to tie down these relative velocities. This equation is commonly referred to as the bootstrap condition (Krishna and Wesselingh, 1997; Taylor and Krishna, 1993).

Flow models

Although, in principle, it is possible to describe almost any kind of flow pattern using exotic cell layout and connection patterns, this article is focused on the influence of vapor and liquid backmixing on distillation trays. The limiting cases that will be considered are illustrated in Figure 3. The simplest, shown on the left of the figure, has both vapor and liquid phases perfectly mixed. In this case the cell description is superfluous, since the stage and cell flows will be the same. This case is, however, not representative of the true flow patterns on a tray. There is general agreement on the assumption that vapor rises in plug flow through the layer of liquid on a stage. In addition it is often assumed that the liquid is well mixed in vertical direction due to the vapor jets and bubbles. The liquid phase may be assumed to be completely well mixed for trays with short flow paths, however, significant staging is to be expected for longer flow path lengths.

The first of these cases in which the vapor rises in plug flow through an ideally mixed pool of liquid is illustrated in the middle of Figure 3. Vertical mixing is established by additional liquid mixing flows, denoted by L^M and represented by the broad arrows. The flow rates of all the mixing streams are assumed to be equal. In the third case, shown on the right-hand side of Figure 3, staging in the liquid flow direction is taken into account by specifying multiple columns of cells. The number of cells needed to model realistic flow patterns may be derived from literature correlations for axial dispersion coefficients (see Lockett, 1986) and Eq. 3. The cell component and enthalpy balances will have to be adjusted to account for the mixing flows.

Because the liquid mixing streams for all cells are assumed to be equal, the overall liquid-phase mass balance for a cell
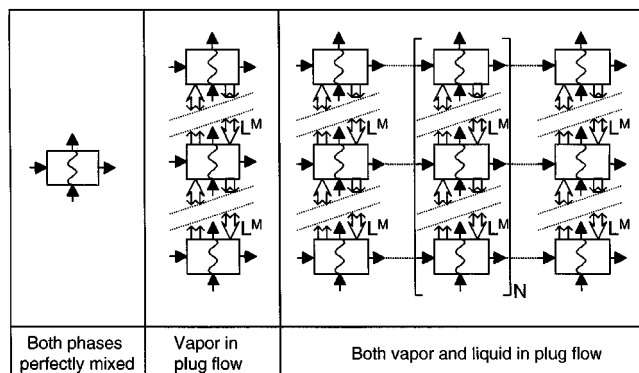
Both phases perfectly mixed	Vapor in plug flow	Both vapor and liquid in plug flow

Figure 3. Cell description of various flow models.

will not change. The modified liquid-phase component balance for an arbitrary cell is given by

$$L^C_{(k,m)} \cdot x^C_{i,(k,m)} - L^C_{(k-1,m)} \cdot x^C_{i,(k-1,m)} - f^{LC}_{i,(k,m)} - \mathfrak{R}^L_{i,(k,m)}$$

$$+ \sum_{l=1}^{r} \nu_{i,l} R_{l,(k,m)} \epsilon_{(k,m)} + L^M$$

$$\cdot \left(2 x^C_{i,(k,m)} - x^C_{i,(k,m-1)} - x^C_{i,(k,m+1)} \right) = 0 \quad (34)$$

Here $x^C_{i,(k,m+1)}$ and $x^C_{i,(k,m-1)}$ are the liquid-phase compositions in the cells above and below the cell under consideration. L^M is the liquid mixing flow rate. This equation differs slightly for the top and bottom cells in a column. The cells in the top row of a stage have liquid exchange only with the cells below. The bottom cells only mix with the cells directly above.

The liquid-phase energy balance for a cell with mixing flows is given by

$$L^C_{(k,m)} \cdot H^{LC}_{(k,m)} - L^C_{(k-1,m)} \cdot H^{LC}_{(k-1,m)} - F^{LC}_{(k,m)} H^{FL}_{(k,m)} + Q^{LC}_{(m,k)}$$

$$- \mathcal{E}^L_{(k,m)} + L^M \cdot \left(2 H^{LC}_{(k,m)} - H^{LC}_{(k,m-1)} - H^{CL}_{(k,m+1)} \right) = 0 \quad (35)$$

The liquid mixing flow has to be large enough to ensure ideal liquid mixing in the vertical direction.

Kooijman (1995) derives and uses an analytical approximation for the mass-transfer rates for this model, but he assumes the vapor interface concentration and the matrix of vapor-phase mass-transfer coefficients to be constant over the froth height. This assumption is legitimate only if the resistance to mass transfer is assumed to be confined entirely to the vapor phase and the liquid phase is well mixed. For the liquid flow model, Kooijman corrects the vapor interface concentration because it is not justifiable to assume a constant vapor interface concentration everywhere on the tray. The changes in interface mole fractions are related to the average liquid mole fraction differences over the mass-transfer film on the tray and at the outlet. The correction factor was chosen by matching numerical calculations to experimental data. These assumptions are not made in the cell model, since mass-transfer coefficients and interface concentrations are calculated for each cell independently.

Reboiler and condenser

The reboiler and condenser will be modeled as equilibrium stages. For each equilibrium stage, the total mass balance is given by

$$L^S_j - L^S_{j-1} + V^S_j - V^S_{j+1} - F_j + \sum_{l=1}^{r} \left(\sum_{i=1}^{c} \nu_{i,l} \right) R_{l,j} \cdot \epsilon_j = 0 \quad (36)$$

The individual component balances are given by

$$L^S_j \cdot x^S_{i,j} - L^S_{j-1} \cdot x^S_{i,j-1} + V^S_j \cdot y^S_{i,j} - V^S_{j+1} \cdot y^S_{i,j+1} - f_{i,j}$$

$$+ \sum_{m=1}^{r} \nu_{i,m} \cdot R_{m,j} \cdot \epsilon_j = 0 \quad (37)$$

The overall energy balance of an equilibrium stage is given by

$$L^S_j \cdot H^{LS}_j - L^S_{j-1} \cdot H^{LS}_{j-1} + V^S_j \cdot H^{VS}_j - V^S_{j+1} \cdot H^{VS}_{j+1}$$

$$- H^F \cdot F_j + Q_j = 0 \quad (38)$$

In addition, phase equilibrium is assumed between the two bulk phases

$$y^S_{i,j} - K_{i,j} x^S_{i,j} = 0 \quad (39)$$

The mole fractions of both phases should sum up to 1. These summation equations may be combined to give

$$\sum_{i=1}^{c} x^S_{i,j} - \sum_{i=1}^{c} y^S_{i,j} = 0 \quad (40)$$

The pressure in the reboiler may be calculated from

$$p_j - p_{j-1} - (\Delta p_{j-1}) = 0 \quad (41)$$

The pressure of the condenser has to be specified

$$p_1 - p_{\text{spec}} = 0 \quad (42)$$

Model System
Variables

The variables for each nonequilibrium stage are listed in Table 1. The total number of stage variables is $(2 \cdot c + 5)$. The total number of cell variables per cell $(6 \cdot c + 5 + n_1 \cdot (2 \cdot c + 1)$

Table 1. Variables for a Nonequilibrium Stage

For the Flow from each Stage		
Flow rates	L^S_j and V^S_j	2
Compositions	$x^S_{i,j}$ and $y^S_{i,j}$	$2 \cdot c$
Temperatures	T^{LS}_j and T^{VS}_j	2
Stage pressure	p_j	1
For the Bulk of each Cell		
Cell flow rates	$L^C_{(k,m)}$ and $V^C_{(k,m)}$	2
Compositions of cells	$x^C_{i,(k,m)}$ and $y^C_{i,(k,m)}$	$2 \cdot c$
Temperatures of cells	$T^{LC}_{(k,m)}$ and $T^{VC}_{(k,m)}$	2
Mass transfer rates	$\mathfrak{R}^C_{i,(k,m)}$	c
For the Liquid Film n_1 Discretization Points		
Composition	$x^C_{i,(k,m)}$	$c \cdot n_1$
Mass transfer rates	$\mathfrak{R}_{i(k,m)}$	$c \cdot n_1$
Temperatures	$T^C_{(k,m)}$	n_1
For the Vapor Film, n_2 Discretization Points		
Composition	$y^C_{i(k,m)}$	$c \cdot n_2$
Temperature	$T^C_{(k,m)}$	n_2
For the Interface		
Composition	$x^{IC}_{i,(k,m)}$ and $y^{IC}_{i,(k,m)}$	$2 \cdot c$
Mass transfer rates	$\mathfrak{R}_{i,(k,m)}$	c
Temperature	$T^C_{(k,m)}$	n_2

Table 2. Variables for an Equilibrium Stage

Stage flows	L_j^S and V_j^S	2
Compositions	$x_{i,j}^S$ and $y_{i,j}^S$	$2c$
Temperatures	T_j^S	1
Stage pressure	p_j	1
Heat duty	Q_j	1

$+ n_2 \cdot (c+1))$. For the simplest system, when just using one cell per stage and just one discretization point in both mass-transfer films, there are $(11 \cdot c + 12)$ variables per stage. The reboiler and condenser (if present) are modeled as equilibrium stages. The variables on the equilibrium stages are summarized in Table 2. For each equilibrium stage, there are $(2 \cdot c + 5)$ variables per stage.

Equations

The equations to be solved for each nonequilibrium stage are listed in Table 3. For each stage, we have $(2 \cdot c + 5)$ equations, and for each cell we have $[6 \cdot c + 5 + n_1 \cdot (2 \cdot c + 1) + n_2 \cdot (c+1)]$ equations. The equations for the reboiler and condenser are listed in Table 4. For each equilibrium stage there are $2c + 4$ equations.

Degrees of freedom analysis

The total number of variables and equations for a c component system in a column of n_s stages, n_c cells per stage, using n_1 discretization points in the liquid film, and n_2 discretization points in the vapor film is: $n_s \cdot (2 \cdot c + 5 + n_c \cdot (6 \cdot c + 5 + n_1 \cdot (2 \cdot c + 1) + n_2 \cdot (c+1)))$.

For the condenser and the reboiler, there are $2 \cdot c + 5$ variables and $2 \cdot c + 4$ equations, resulting in one degree of free-

Table 3. Equations for a Nonequilibrium Stage

For Each Stage		
Total mass conservation eqs.	Eqs. 4 and 5	2
Component conservation eqs.	Eqs. 6 and 7	$2 \cdot c$
Total energy conservation eqs.	Eqs. 8 and 9	2
Hydraulic equation	Eq. 10	1
For Each Cell		
Total mass conservation eqs.	Eqs. 11 and 12	2
Total component conservation eqs.	Eqs. 15 and 16	$2 \cdot c$
Total energy conservation eqs.	Eqs. 17 and 18	2
For the Liquid Transfer Film		
Mass-transfer correlations	Eq. 19	$(c-1) \cdot (n_1 + 1)$
Summation eqs.	Eq. 21	n_1
Species conservation eqs.	Eq. 23	$c \cdot (n_1 + 1)$
Energy transfer eqs.	Eq. 26	n_1
For the Vapor Transfer Film		
Mass-transfer correlations	Eq. 20	$(c-1) \cdot (n_2 + 1)$
Summation eqs.	Eq. 22	n_2
Energy transfer eqs.	Eq. 27	n_2
For the Interface		
Interface equilibrium eqs.	Eq. 28	c
Interface summation eqs.	Eqs. 30 and 31	2
Bootstrap eq.	Eq. 33	1

Table 4. Equations for an Equilibrium Stage

Total mass conservation eq.	Eq. 36	1
Total component conservation eq.	Eq. 37	c
Total energy conservation eq.	Eq. 38	1
Equilibrium eqs.	Eq. 39	c
Summation eq.	Eq. 40	1
Pressure eq.	Eq. 41 or 42	1

dom for each such stage. The energy balance is replaced by a specification equation on, for example, the reflux ratio, the bottom product flow rate, and so on.

The additional specifications required for a complete column simulation with the new nonequilibrium model are detailed below.

Configuration. The configuration of the column needs to be fixed. This requires specification of the number of trays, reboiler type (if any), condenser type (if any), and the number of feeds and their locations with the number and location of any sidestreams and the external heat duties (if any).

Pressure Model and Condenser Pressure. The condenser pressure has to be specified. In addition it is common practice to give an independent specification for the pressure of the top stage, as, depending on the design, the top stage pressure may be very different from the condenser pressure. Furthermore, a pressure drop model for the nonequilibrium stages is required. Possible options are:

(1) Zero pressure drop. All stages in the column operate at the specified top stage pressure.

(2) Fixed pressure drop. The stage pressure drop is specified. The stage pressure is evaluated using Eq. 10.

(3) Fixed Bottom pressure. With the top and bottom pressures fixed, the pressures on all other stages are evaluated by means of interpolation.

(4) Estimated pressure drop. A value for the pressure drop is estimated from a semiempirical correlation.

For bubble cap trays, the correlation due to Bolles and Smith (1963) is used; for sieve trays, the correlation due to Bennett et al. (1983) is used. The stage pressure is evaluated using Eq. 10.

Feeds. Specification of the flow rate, composition, and thermodynamic state of each feed is required. The latter can be determined after specification of any two of the following three parameters: temperature, pressure, and vapor fraction.

Thermodynamic Models and Physical Properties. Specification of a thermodynamic model is required for the calculation of, among other things, vapor-liquid equilibrium ratios, reaction rates, enthalpies, and chemical potential gradients. In addition, a nonequilibrium model requires information about physical properties, such as surface tension, density and heat capacity, for evaluation of parameters such as the mass-transfer coefficients, pressure drops, and interfacial areas. A more complete listing of the available property models can be found in Taylor et al. (1994).

Design. Some of the quantities appearing in the equations given above depend on the internals design and configuration (pressure drop, vapor-liquid interfacial area, reaction volume, and mass- and heat-transfer coefficients). This inevitable link between design and model equations is discussed extensively by Taylor et al. (1994), and they point out

that the nonequilibrium model can only be used for an existing column. To alleviate this problem, they proposed an integration of a design procedure together with the model equations. During the calculations, a design is evaluated based on calculated liquid and vapor flows and physical properties. The same approach is adopted in our model. For more details about the design mode, see Taylor et al. (1994) and Kooijman (1995). At the very least, one is required to specify the internals type, although specification of detailed designs remains a possibility.

Mass- and Heat-Transfer Model. The binary pair mass-transfer coefficients are calculated from empirical correlations (Taylor and Krishna, 1993). In the calculations presented in this article, the AIChE (1958) correlation was used. For calculation of the vapor-phase heat-transfer coefficients, the Chilton-Colburn analogy between mass and heat transfer is used. For the calculation of the liquid heat-transfer coefficients, the penetration theory is used.

Reaction. A reaction rate expression along with kinetic parameter data are required for evaluation of the reaction rates. For calculation of the reaction volume in heterogeneous systems, the total catalyst mass present on a stage, and the catalyst activity, have to be specified. For a homogeneous system, the reaction can take place in the liquid bulk and in the liquid transfer film. The reaction volume of the liquid bulk is taken to be the total liquid inventory on a tray. This is obtained by multiplying the clear liquid height by the active tray area. The clear liquid height is calculated from the semi-empirical correlation due to Bennet et al. (1983). The film volume is the product of the interfacial area and the liquid film thickness, which is obtained from

$$\delta^L = \frac{\bar{\kappa}}{\overline{\overline{D}}} \qquad (43)$$

In which $\bar{\kappa}$ and $\overline{\overline{D}}$ are average values for the binary pair mass-transfer and diffusion coefficients.

Steps and Cells. The following degrees of freedom result from the cell description:
- Number of cells in a liquid flow branch
- Number of cells in a vapor flow branch
- Number of discretization steps in the liquid film
- Number of discretization steps in the vapor film
- Mixing flow rate.

The number of cells in both flow paths depends on the flow model under consideration. The appropriate number of cells depends on the configuration and operating conditions used. In a column simulation, one would typically first do column calculations without assuming staging in the liquid flow direction. From these calculations, one can obtain information about the hydrodynamic conditions on the stages. These can be used to evaluate an axial dispersion coefficient, employing a semi-empirical correlation. These axial dispersion coefficients can be used to estimate the number of cells required for description of flow behavior on a distillation tray. The vapor flow is normally assumed to be in plug flow and may be modeled by using at least five cells in the vapor flow direction.

The vertical liquid mixing flow rate should be such that the bulk liquid concentrations of all cells in a vapor foot path are

equal. This is usually satisfied if the mixing flow rate is taken to be three to four times the stage flow rate.

In choosing the number of discretization steps we would like to combine accuracy and calculation speed. In nonreactive systems, where concentration gradients are typically not very large, one or two discretization points in both the vapor- and liquid-transfer films are usually sufficient. In these cases, the model by Kooijman and the model presented here give the same results. For systems with reactions, or for systems with strong thermal effects in mass transfer, more points should be specified.

Solving the model equations

Newton's method is used for solving the model equations. Details of the implementation are essentially as described by Taylor et al. (1994).

Simple Distillation Column

To test the cell model, we have done some simulations for a depropanizer as described in detail by Kooijman and Taylor (1995). The number of discretization points in the vapor- and liquid-transfer films was set to five. Assuming both vapor and liquid are perfectly mixed, both models give identical results.

Calculations were also done for the depropanizer to determine the number of cells needed to adequately describe plug flow in the vapor. Theoretically, the number of cells in this the vertical direction should go to infinity. However, our calculations suggest that the changes in column behavior due to adding cells are very small after the fifth cell. Plug flow in the liquid phase is only achieved when the number of cells in the liquid flow direction goes to infinity. As was observed above, changes in column behavior due to additional cells are very small after adding the fifth column. Differences between Kooijman's model and the presented model can be attributed to the different interface descriptions, as discussed above. Differences between the cell model and Kooijman's model can be attributed to the different interface descriptions. In Kooijman's model the interface concentration is fixed over the froth height. We find that the interface concentration may change by up to 50% of its average value over the froth height for species that have a relatively low concentration.

Reactive System

One of the principal reasons for the development of the third generation nonequilibrium model, described in this article, is to be able to model reactive separation processes more accurately. Some preliminary results obtained with this model are presented by Higler et al. (1998, 1999a,b).

We will use a reactive system that is similar to one considered by Okasinski and Doherty (1998) to test the influence of the flow patterns. The following reaction takes place

$$2A \rightarrow B + C \qquad (44)$$
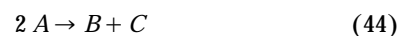
A typical reaction system fitting this scheme is the metathesis reaction of 2-pentene to 3-hexene and 2-butene. Physical and thermodynamic properties of this system will be used

in the remainder of the calculations. Reaction kinetic data were taken from Hughes (1970). The overall reaction rate is given by (Okasinski and Doherty, 1998)

$$R_i = \nu_i \cdot \left(k_\rightarrow \cdot x_{c5}^2 - k_\leftarrow \cdot x_{c4} \cdot x_{c6}\right) \qquad (45)$$

with the following rate constants

$$k_\rightarrow = 78.2 \cdot e^{-(27.6 \cdot 10^3/\Re \cdot T)}[s^{-1}] \qquad (46)$$

and

$$k_\leftarrow = 312.8 \cdot e^{-(27.6 \cdot 10^3/\Re \cdot T)}[s^{-1}] \qquad (47)$$

We have chosen to use the following configuration: A 25-stage column with a liquid feed of pure 2-pentene to stage 13 (counting from the top). The feed rate is fixed at 10 mol/s. The condenser and column top pressure are fixed at 101.3 kPa, while the stage pressure drop is calculation due to Bennett et al. (1983). The top product flow rate was fixed to half the feed rate. The boilup ratio was varied in a parametric study, as was the number of cells. For calculation of thermodynamic properties, the Peng-Robinson equation is used. Reaction rates are calculated using the kinetic expressions as given by Eq. 45 to Eq. 47. Mass-transfer coefficients are evaluated using the AIChE (1958) method.

Calculations

Calculations were done for the above column in which the boilup ratio was varied from five to ten. The cell configurations used were: (1) A single cell per stage (corresponding to both phases perfectly mixed), (2) a single column of cells (approximating vapor plug flow through a well mixed pool of liquid), and (3) multiple columns of cells (approximating vapor rising in plug flow through the liquid in plug flow across the tray).

All calculations were done in design mode, using single pass sieve trays with conventional downcomers. The calculated column diameters range between 1 m for a boil-up ratio of five and 1.3 m for a reflux ratio of ten. The calculated flow path lengths range between 0.78 m and 0.91 m. Figure 4 shows the conversion of butene as a function of the reflux ratio for the three flow models. The differences between the models are quite substantial, especially since reactive distillation is a high purity business. The best performance is obtained with cell configuration three. Increasing the reflux ratio should be avoided at all cost since it will require a larger column and additional reboiler and condenser duties.

Cells or not

It would be useful to know if this very detailed way of describing the reaction and mass-transfer processes is really required. The calculations become substantially more time consuming on adding more and more cells. Thus, we need to determine the exact influence of the cell description on the overall production rate, particularly for the liquid flow models. Two different effects need to be separated here. First, there is the effect of staging in the liquid flow direction on
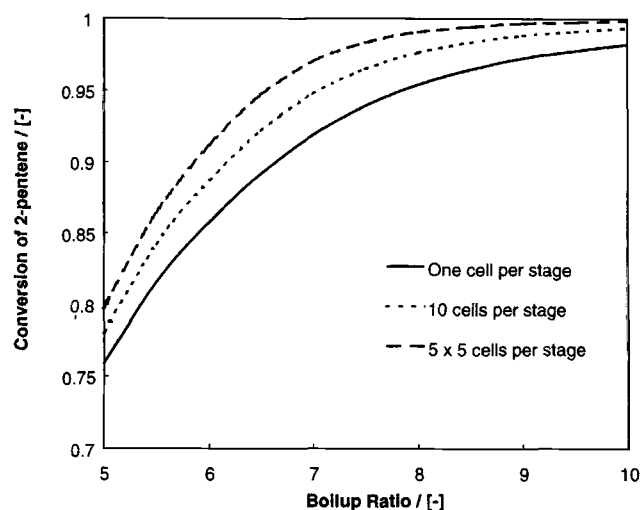

Figure 4. Conversion as a function of boilup ratio for various flow models.

mass transfer, and, secondly, the effect of staging on the local concentrations along the liquid flow path, and, through that, on the production rates. If the influence of the latter is not significant, a much smaller model may give usable results.

Such a smaller model may be obtained by extending the model of Kooijman and Taylor (1995) to take into account chemical reactions. Assuming the reaction takes place only in the bulk liquid, only the overall mass and component balances for the liquid phase have to be modified. This implicitly assumes there is no direct interaction between mass transfer and reaction.

Figure 5 shows the conversion of 2-pentene as a function of the reflux ratio, assuming vapor and liquid plug flow, for both models. The differences are small and will, in the high conversion region, fall within the range of accuracy for both models. Although the simplified model has some fundamental weaknesses, it may in some cases offer a fast alternative to
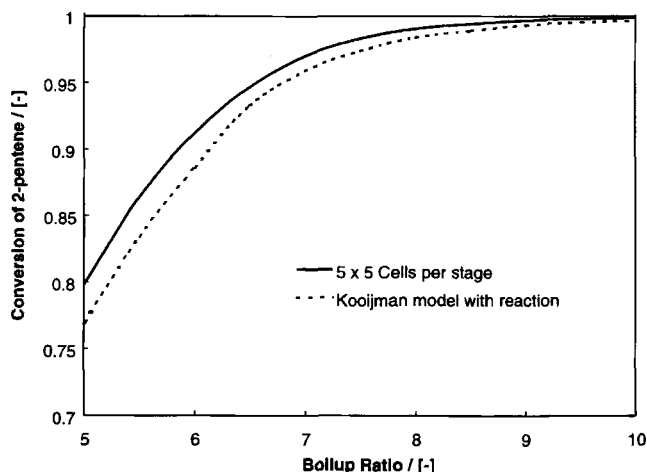

Figure 5. Comparison of cell model to modified Kooijman (1995) model extended with bulk liquid reaction.

the cell model. Some caution is in order however: The simplified model should not be used for systems in which very fast reactions occur, such as acid gas stripping. In such cases mass transfer is very strongly influenced by the reaction.

Nonequilibrium model vs. equilibrium model

Based on the previous observations, one might argue that it is possible to save even more calculation time by reverting to an equilibrium stage approach. There are, however, some objections to this approach. The most important one is the fact that there is no correct way of linking a theoretical equilibrium stage to a real tray. This is normally done by means of an efficiency factor, and the most commonly used is the Murphree vapor phase efficiency defined by

$$E^{MV} = \frac{y_{i,j} - y_{i,j+1}}{y_{i,j}^* - y_{i,j+1}} \tag{48}$$

in which $y_{i,j+1}$ is the composition of the vapor below the tray, $y_{i,j}$ is the composition of the vapor above the tray, and $y_{i,j}^*$ is the concentration of vapor that would be in equilibrium with the liquid bulk on the tray. This may be replaced by $K_i \cdot x_{i,j}$ to give

$$E^{MV} = \frac{y_{i,j} - y_{i,j+1}}{K_i \cdot x_{i,j} - y_{i,j+1}} \tag{49}$$

The liquid-phase mole fraction will not only change due to mass transfer, but also due to the reaction. Figure 6 shows the actual efficiency profiles, back-calculated from column concentration profiles obtained with the nonequilibrium model. Although it is a well known fact that in multicompo-
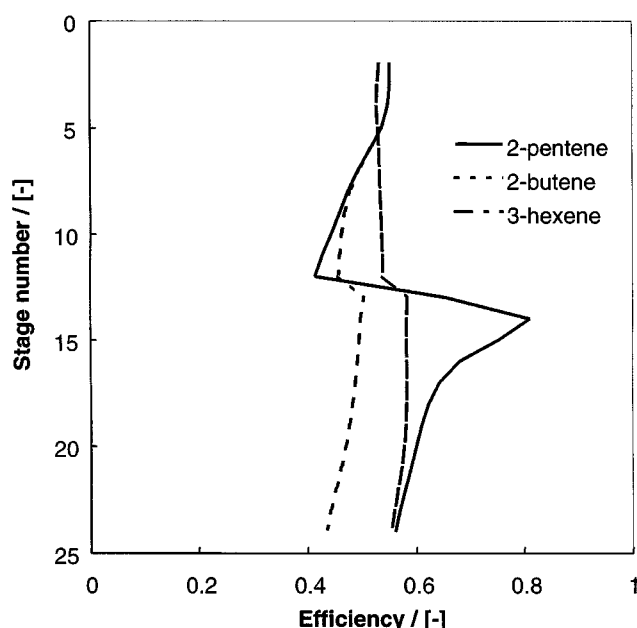
nent systems these efficiencies tend to misbehave, there are a few remarkable things to the profiles in Figure 6.

The efficiencies of pentene just above the feed are much higher than just below the feed. This is due to the fact that, above the feed, pentene is a relatively heavy component, and, below the feed, it is relatively light. Furthermore, it is a reactant. Below the feed, where pentene is relatively light, the vapor-phase concentration on the tray above will be larger than the vapor-phase concentration of the tray below. This means that the numerator of Eq. 48 will be larger than zero. The same will usually be the case for the denominator. However, because it is reactant, there will be consumption of pentene, lowering its mole fraction. This means that the numerator will be smaller than for a system without a reaction, resulting in higher measured efficiencies. Similar considerations can be given for the rectifying section. The result of all this is that if component i is a reactant and is relatively light, the measured efficiency will be higher than normal. However, if component i is a reactant but now relatively heavy, the measured efficiency will be lower than normal.

Similar considerations apply to products. For a relatively light product, lower efficiencies are to be expected, and for a heavy product we expect to see a higher efficiency. Clearly, the efficiencies are reaction dependent, which makes them difficult to predict. Using an efficiency model for a reactive distillation column is, therefore, not recommended.

Acetic Anhydride Reactive Distillation

The first work in the field of integrating a liquid flow model in a numerical model for a reactive distillation column was by Alejski (1991), who modeled the system water, acetic anhydride, and acetic acid. The modeled column was part of a plant for the production of acetic anhydride described by Marek (1956). The objective of the column is to separate water and acetic anhydride to avoid hydrolysis of the anhydride to acetic acid. Conversion of acetic anhydride should be avoided as much as possible.

Alejski uses a model in which the liquid phase on a tray is split up in a number of equilibrium cells along the liquid flow path. To take into account mass-transfer effects, locally evaluated point efficiencies are used in the phase equilibrium calculation of each cell. The number of cells was evaluated from expressions for the eddy diffusivity. Alejski found that the conversion of anhydride as calculated assuming a perfectly mixed liquid phase was higher than when assuming that the liquid flows in plug flow across the tray. The numerical model was tested against experimental data for a bubble cap column of 0.6 m diameter, containing 30 bubble cap trays, with a total height of 10 m (Marek, 1956).

Reaction

The reaction equation is

$$(CH_3CO)_2O + H_2O \rightarrow 2CH_3COOH \tag{50}$$
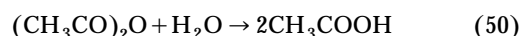
The reaction is assumed to be irreversible and the reaction rate equation is given by

$$r = k_c \cdot c_{(CH_3CO)_2O} \cdot c_{H_2O} \tag{51}$$

Figure 6. Efficiency profiles for reactive system calculated from nonequilibrium model results.

Table 5. Feed Properties for Acetic Anhydride Column

Pressure	53.0 kPa
Temperature	290 K
Flow rate	0.92 mol/s
Component Mole Fractions	
Acetic anhydride	0.161
Water	0.484
Acetic acid	0.355

The reaction rate constant is given by Marek (1956)

$$\ln(k_c) = 11.742 - \frac{6,887.7}{T} \qquad (52)$$

Configuration

The column has 30 trays with a total condenser and a partial reboiler (a total of 32 stages) with a feed to stage 16. The column diameter was set to 0.6 m during the calculations. The condenser pressure is 53.0 kPa. The reboiler pressure is 54.2 kPa. The column is operated at a reflux ratio of 5.18 and a bottom product flow rate of 0.43 mol/s. Feed specifications are given in Table 5.

Thermodynamic data

A limited quantity of vapor-liquid equilibrium data is provided by Marek (1956). These data were obtained only in a very small region of the ternary triangle, that is, nevertheless, representative of the compositions observed in the actual column. We have correlated these data with the Wilson equation, for which the relative differences between the experimental and calculated V/L-equililbrium compositions were minimized. The parameters used here are given in Table 6.

Calculations

Calculations were made for the above system with our nonequilibrium model. With the specifications given above, the trays operate at a flooding fraction of about 0.18. This operating point falls outside the range of applicability of all published hydrodynamic correlations. This means that the predictions for parameters such as the interfacial areas, clear liquid heights, and mass-transfer coefficients will not be reliable, and may have to be adjusted to fit the experimental data. Initial calculations suggest that an acceptable fit of experimental data was obtained by multiplying the estimated clear liquid height by 0.4 and the estimated mass-transfer coefficients by 0.5. Subsequent calculations were done for the three different flow models described above. Concentration profiles are presented in Figure 7. The shift in the concentra-
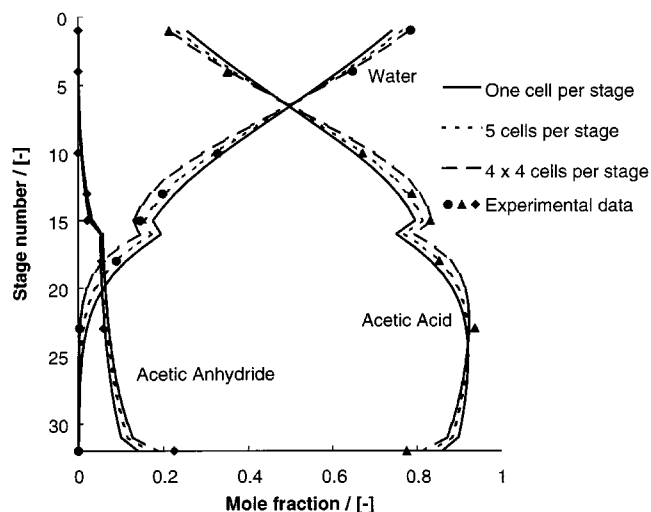

Figure 7. Column concentration profiles for acetic anhydride-water-acetic acid system.

tion profiles due to increased staging in the vapor and liquid flow paths follows the trends as observed by Alejski. Table 7 shows that there is a drop in conversion with increased staging in liquid and vapor flow directions. This should be no surprise from a mass-transfer perspective. In the system under consideration, water is the lightest and acetic anhydride is the heaviest component. The mass-transfer rates for each species are shown in Figure 8. In the top section, where the mixture consists mostly of water and acetic acid, we see that increased staging leads to a higher rate of transfer of water from the liquid to the vapor phase (negative direction). At the same time, there is increased transfer of acetic acid from the vapor to the liquid phase (positive direction). Similar behavior is seen at the feed stage.

Below the feed stage, however, the trends are reversed. Here, staging seems to reduce the mass-transfer rate of water. The reason for this is offered by the concentration profiles. Due to the improved performance of the top section, there is not much water left below the feed stage. Thus, the mass-transfer rates drop due to staging. In the bottom stages of the column, acetic acid moves from the liquid into the vapor phase, while acetic anhydride moves from the vapor into the liquid phase. Here, increased staging leads to higher mass-transfer rates and improved performance.

As a result, the concentrations of water and acetic anhydride will be lowered in the center of the column, thereby reducing the reaction rate and the consumption of acetic anhydride. The consumption rate of acetic anhydride is shown in Figure 9. The expected effects are clearly visible. Particularly below the feed stage, the consumption rate has dropped considerably, due to the lower concentration of water.

Table 6. Wilson Parameters Acetic Anhydride–Water–Acetic Acid System

Component i	Component i	$a_{i,j}$ (J/mol)	$a_{j,i}$ (J/mol)
Acetic anhydride	Water	2,214.3	5,024.6
Acetic anhydride	Acetic acid	−407.2	3,323.7
Water	Acetic acid	4,714.4	−4,062.78

Table 7. Conversion of Acetic Anhydride for Various Flow Models

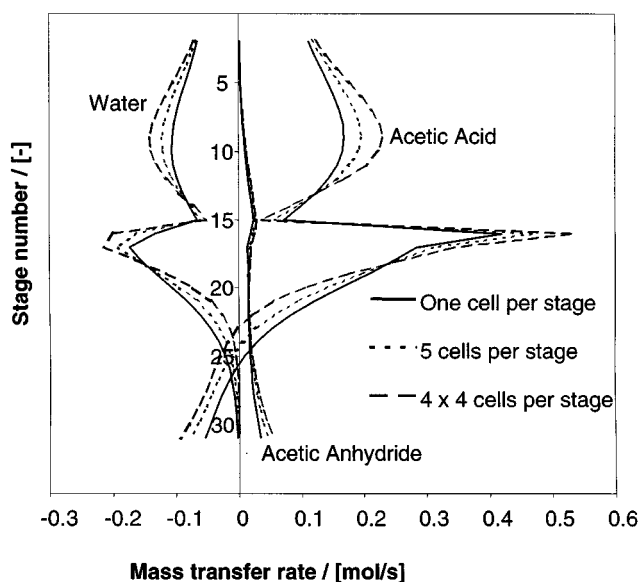|	
1 Cell	0.58
5 Cells (vapor plug flow)	0.51
4×4 Cells (vapor and liquid plug flow)	0.45

Figure 8. Column mass-transfer rate profiles for acetic ahydride-water-acetic acid system.

Conclusion

We have developed a generic nonequilibrium cell model for multicomponent (reactive) distillation tray columns. Important model features are the use of the Maxwell-Stefan theory for the description of interphase mass transfer, the use of a multiple cell per stage approach for the description of various flow models, and the possibility of incorporating reactions.

A finite difference approach was used for solving the Maxwell-Stefan equations. This was done in order to be able to take directly into account the effects of reactions on mass

Figure 9. Consumption rate of acetic anhydride.

transfer. The multiple cells per stage approach was adopted to be able to take into account the effect of local concentration and temperature profiles on a tray on the local reaction rates.

The nonreactive model was tested with case studies described by Kooijman (1995). It was found that the influence of the number of discretization points for the infinite difference approximation of the Maxwell-Stefan equations was not significant for these systems. In these cases, concentration profiles are not very steep and the use of one discretization point gave very good results in all nonreactive cases. This may not be true for reactive systems. Reactions can influence the concentration profiles significantly and caution should be used when specifying a number of discretization points. This is especially true for systems with very fast reactions.

The cell approach to flow pattern modeling was tested by comparison to the model presented by Kooijman. Here only minor differences were found between Kooijman's model and the nonequilibrium cell model. These differences were only found for cases in which it was assumed that the phases are not perfectly mixed. This is due to the different interface concentration descriptions for the various flow models. In his vapor plug-flow model, Kooijman assumes that the interface mole fractions of the various components do not change over the height of the froth. We have found a change of as much as 50% in some cases.

In addition, calculations were presented for two reactive systems. In both cases, a significant influence of staging in both vapor and liquid flow paths was found.

There is a growing body of evidence that suggests that nonequilibrium models are capable of superior predictions of actual column behavior compared to efficiency-modified equilibrium stage models. The nonequilibrium models of Krishnamurthy and Taylor (1985) and of Taylor et al. (1994), as well as equilibrium stage models, are special cases of the more general model developed here. Thus, the present model is capable of predicting the performance of actual columns at least as well as these earlier models.

Notation

a = interfacial area, m^2
c = total number of components
$Đ$ = Maxwell-Stefan diffusion coefficient, $m^2 \cdot s^{-1}$
D_e = axial dipersion coefficient, $m^2 \cdot s^{-1}$
E^{MV} = Murphree vapor-phase efficiency
$\mathcal{H}_i^L$ = partial molar liquid enthalpy of component i, $J \cdot mol^{-1}$
$\mathcal{H}_i^V$ = partial molar vapor enthalpy of component i, $J \cdot mol^{-1}$
k_c = concentration based reaction rate constant, $m^3 \cdot mol^{-1} \cdot s^{-1}$
$k_{m,\rightarrow}$ = forward reaction rate constant reaction m, $mol \cdot m^{-3} \cdot s^{-1}$
$k_{m,\leftarrow}$ = backward reaction rate constant reaction m, $mol \cdot m^{-3} \cdot s^{-1}$
n_c = number of cells per stage
n_s = number of stages
n_1 = number of discretization points in the liquid film
n_2 = number of discretization points in the vapor film
Pe = Peclet number
r = total number of reactions
$x_{i,j}^S$ = liquid mole fraction of component i on stage j
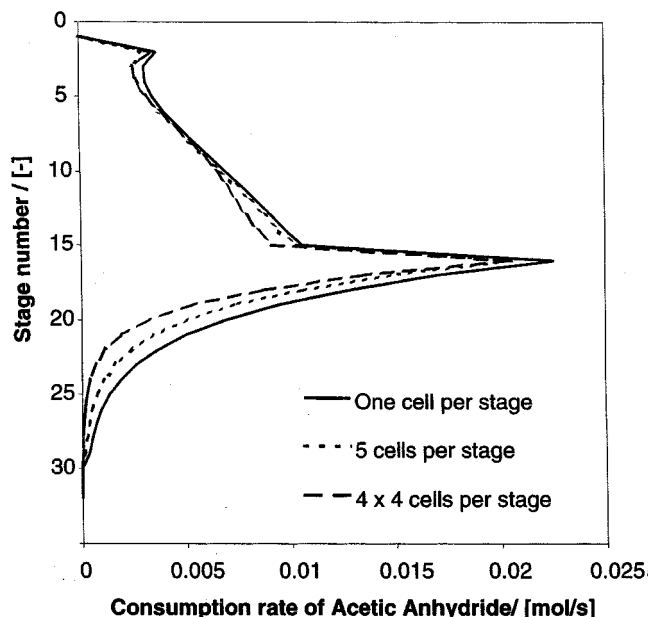$y_{i,j}^S$ = vapor mole fraction of component i on stage j
z = coordinate direction

γ_i = activity coefficient of component i
Γ = thermodynamic factor
δ = film thickness, m
$\delta_{i,k}$ = Kronecker delta, 1 of $i = k$, 0 if $i \neq k$
$\kappa_{i,l}$ = binary pair mass-transfer coefficient components i and j, m·s^{-1}

Superscripts

$*$ = indicating equilibrium
$-$ = averaged value
C = cell quantity or property
F = feed quantity or property
I = interface quantity or property
L = liquid phase quantity or property
M = mixing flows
MV = Murphree vapor phase
S = stage quantity or property
V = vapor phase quantity or property

Subscripts

I = evaluated at interface
c_4 = butene
c_5 = pentene
c_6 = hexene
(k,m) = cell index
l = reaction index
spec = specification
t = total

Literature Cited

AIChE, *Bubble Tray Design Manual, Prediction of Fractionation Efficiency*, AIChE, New York (1958).

Alejski, K., "Computation of the Reacting Distillation Column Using a Liquid Mixing Model on the Plates," *Comput. Chem. Eng.*, **15**, 313 (1991).

Barker, P. E., and M. F. Self, "The Evaluation of Liquid Mixing Effects on a Sieve Plate Using Unsteady and Steady State Tracer Techniques," *Chem. Eng. Sci.*, **17**, 541 (1962).

Bennett, D. L., R. Agrawal, and P. J. Cook, "New Pressure Drop Correlation for Sieve Tray Distillation Columns," *AIChE J.*, **29**, 434 (1983).

Bennett, D. L., and H. J. Grimm, "Eddy Diffusivity for Distillation Sieve Trays," *AIChE J.*, **37**, 589 (1991).

Bolles, W. L., "Design of Equilibrium Stage Processes," Chapter 14, B. D. Smith, ed., McGraw-Hill, New York (1963).

Gautreaux, M. F., and H. E. O'Connell, "Effect of Length of Liquid Path on Tray Efficiency," *Chem. Eng. Prog.*, **51**, 232 (1955).

Higler, A. P., R. Taylor, and R. Krishna, "Modeling of a Reactive Separation Process Using a Nonequilibrium Stage Model," *Comput. Chem. Eng.*, **22**, S111 (1998).

Higler, A. P., R. Taylor, and R. Krishna, "The Influence of Mass Transfer and Liquid Mixing on the Performance of a Tray Column for Reactive Distillation," *Chem. Eng. Sci.*, **54**, 2873 (1999a).

Higler, A. P., R. Taylor, and R. Krishna, "Nonequilibrium Modeling of Reactive Distillation: Multiple Steady States in MTBE Synthesis," *Chem. Eng. Sci.*, **54**, 1389 (1999b).

Hughes, W. B., "Kinetics and Mechanism of Homogeneous Olefin Disproportionation Reaction," *J. Amer. Chem. Soc.*, **92**, 532 (1970).

Johnson, A. I., and J. Marangozis, "Mixing Studies of a Perforated Distillation Plate," *Can. J. Chem. Eng.*, **36**, 161 (1958).

Kirschbaum, E., "Efficiency of Rectification and Appropriate Path for Liquid Flow," *Forsch. Gebiete Ingenieur*, **5**, 245 (1934).

Kirschbaum, E., *Distillation and Rectification*, Chemical Publishing Co., New York (1937).

Kister, H. Z., *Distillation Design*, McGraw-Hill, New York (1992).

Kooijman, H. A., "Dynamic Nonequilibrium Column Simulation," PhD Diss., Clarkson University, Potsdam, NY (1995).

Kooijman, H. A., and R. Taylor, "On the Estimation of Diffusion Coefficients in Multicomponent Liquid Systems," *Ind. Eng. Chem. Res.*, **30**, 1217 (1991).

Kooijman, H. A., and R. Taylor, "Modelling Mass Transfer in Multicomponent Distillation," *Chem. Eng. J.*, **57**, 177 (1995).

Kreul, L. U., A. Gorak, and P. I. Barton, "Modeling of Homogenous Reactive Separation Processes in Packed Columns," *Chem. Eng. Sci.*, **54**, 19 (1999).

Krishna, R., and J. A. Wesselingh, "The Maxwell-Stefan Approach to Mass Transfer," *Chem. Eng. Sci.*, **52**, 861 (1997).

Krishnamurthy, R., and R. Taylor, "A Nonequilibrium Stage Model of Multicomponent Separation Processes: 1. Model Description and Method of Solution," *AIChE J.*, **31**, 449 (1985).

Lee, J.-H., and M. P. Dudukovic, "A Comparison of the Equilibrium and Nonequilibrium Models for a Multi-Component Reactive Distillation Column," *Comput. Chem. Eng.*, **23**, 159 (1998).

Lewis, W. K., "Rectification of Binary Mixtures," *Ind. Eng. Chem.*, **28**, 399 (1936).

Lockett, M. J., *Distillation Tray Fundamentals*, Cambridge University Press, Cambridge (1986).

Marek, J., "Rectification with a Chemical Reaction: II. Plant Rectification of a Water-Acetic Acid-Acetic Anhydride Mixture," *Coll. Czech. Chem. Commun.*, **21**, 1561 (1956).

McCabe, W. L., and E. W. Thiele, "Graphical Design of Fractionating Columns," *Ind. Eng. Chem.*, **17**, 605 (1925).

Okasinski, M. J., and M. F. Doherty, "Design Method for Kinetically Controlled, Staged Reactive Distillation Columns," *Ind. Eng. Chem. Res.*, **37**, 2821 (1998).

Ponchon, M., "Application of Graphs to the Study of Commercial Fractional Distillation," *Tech Moderne*, **13**, 55 (1921).

Raper, J. A., W. V. Pinczewski, and C. J. D. Fell, "Liquid Passage on Sieve Trays Operating in the Spray Regime," *Chem. Eng. Res. Des.*, **62**, 111 (1984).

Seader, J. D., "The Rate-Base Approach for Modeling Staged Separations," *Chem. Eng. Prog.*, **85**, 41 (1989).

Seader, J. D., "Computer Modeling of Chemical Processes," AIChE Monograph Series **15**(18) (1985).

Sohlo, J., and S. Kinnunen, "Dispersion and Flow Phenomena on a Sieve Plate," *Trans IChemE*, **55**, 71 (1977).

Sorel, E., *Distillatión et Rectification Industrielle*, Carrie and Naud, Paris (1899).

Sundmacher, K., and U. Hoffmann, "Multicomponent Mass and Energy Transport on Different Length Scales in a Packed Reactive Distillation Column for Heterogeneously Catalysed Fuel Ether Production," *Chem. Eng. Sci.*, **49**, 4443 (1994).

Sundmacher, K., "Reactivdestillation mit katalytischen Füllkörperpackungenein neuer Prozeßzur Herstellung der Kraftstoffkomponente MTBE," PhD Diss., Technischen Universität Claustahl, Claustahl Zellerfeld, Germany (1995).

Taylor, R., H. A. Kooijman, and J.-S. Hung, "A Second Generation Nonequilibrium Model for Computer Simulation of Multicomponent Separation Processes," *Comput. Chem. Eng.*, **18**, 205 (1994).

Taylor, R., H. A. Kooijman, and M. R. Woodman, "Industrial Applications of a Nonequilibrium Model of Distillation and Absorption Operations," *IChemE Symp. Ser.*, **128**, A415 (1992).

Taylor, R., and R. Krishna, *Multicomponent Mass Transfer*, Wiley, New York (1993).

Wijn, E. F., "The Effect of Layout Pattern on Tray Efficiency," *Chem. Eng. J.*, **63**, 167 (1996).